

A Modeling of a Lithium Iron Phosphate Battery Using PSCAD

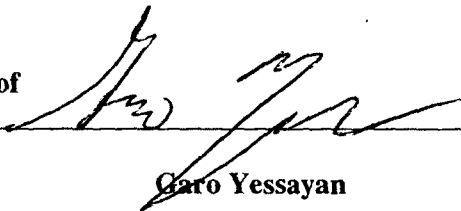
BY

GARO H. YESSAYAN

B.S.E.E UNIVERSITY OF MASSACHUSETTS LOWELL (2011)

SUBMITTED IN PARTIAL FULFILLMENT OF THE REQUIREMENTS  
FOR THE DEGREE OF MASTER OF SCIENCE  
DEPARTMENT OF ELECTRICAL ENGINEERING  
UNIVERSITY OF MASSACHUSETTSLOWELL

Signature of  
Author:



Date:

5/4/12

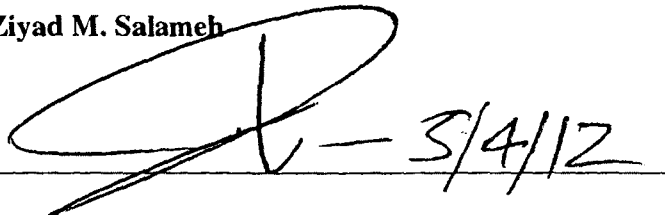
Garo Yessayan

Signature of Thesis Supervisor:



Ziyad M. Salameh

Other Thesis Committee Member Signature:



Prof. MufeedMah'd

Other Thesis Committee Member Signature:



Prof. Joel Therrien



**A Modeling of a Lithium Iron Phosphate Battery Using PSCAD**

**BY**

**GARO H. YESSAYAN**

**ABSTRACT OF A THESIS SUBMITTED TO THE FACULTY OF THE  
DEPARTMENT OF ELECTRICAL AND COMPUTER ENGINEERING  
IN PARTIAL FULFILLMENT OF THE REQUIREMENTS**

**FOR THE DEGREE OF  
MASTER OF SCIENCE  
UNIVERSITY OF MASSACHUSETTS LOWELL  
2012**

**Thesis Supervisor: Ziyad M. Salameh, Ph.D.  
Full Professor, Department of Electrical and Computer Engineering**

UMI Number: 1521360

All rights reserved

INFORMATION TO ALL USERS

The quality of this reproduction is dependent upon the quality of the copy submitted.

In the unlikely event that the author did not send a complete manuscript and there are missing pages, these will be noted. Also, if material had to be removed, a note will indicate the deletion.

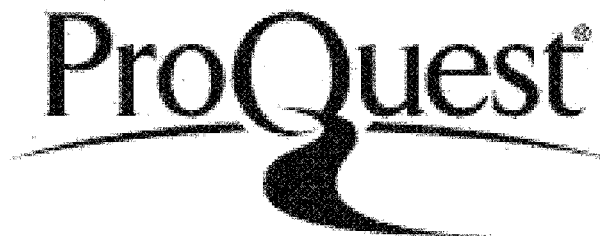


UMI 1521360

Published by ProQuest LLC 2012. Copyright in the Dissertation held by the Author.

Microform Edition © ProQuest LLC.

All rights reserved. This work is protected against unauthorized copying under Title 17, United States Code.



ProQuest LLC  
789 East Eisenhower Parkway  
P.O. Box 1346  
Ann Arbor, MI 48106-1346

## Abstract

Presently, internal combustion engine vehicles (ICEV) are very harmful to humans and the environment. This issue yields a large problem for our society and has helped revolutionize the study of electric vehicles. Although electric vehicles are pollution free, there are two main concerns in their development; the first being the charging and discharging characteristics of the total battery performance and the second being the range. Due to this, battery development is a crucial aspect to improving the performance of electric vehicles.

This progress requires dependable computer aided designs to model the battery accurately and reliably. Using Power Systems Computer Aided Design (PSCAD) the qualities of a constant discharging Lithium Iron Phosphate battery was observed by creating an equivalent runtime circuit model. This model demonstrates the performance effects of the lithium iron phosphate battery given varying temperatures and battery state of charge (SOC). The runtime model constitutes of two circuits. The first circuit represents the change in SOC over a period of time by implementing a dependent current source and a resistor in series. In addition to this, the runtime model includes a second circuit that mimics the Thevenin model using multiple parallel R-C networks that are in series with the dependent voltage source. All the parameters are based on the SOC.

In order to find the fixed parameters of the circuit, MATLAB was used to implement basic current voltage characteristics. The collected data for various temperatures was inserted into MATLAB and organized with the intent to find a model of the terminal voltage ( $V_t$ ) of the battery. Given the varying SOC multiple equations were

determined for the variable battery voltage, and were the deciding factors in obtaining the component values of the modeled circuit. Once these parameters were found, the circuit was simulated in PSCAD.

In order for the PSCAD simulator to function properly it was necessary that the SOC varied with time. Given a 160 Ah Lithium Iron Phosphate battery, a circuit was created that showed a graphical output of a varying SOC for 7200 seconds or 2 hours. The second circuit was created using mathematical simulators in PSCAD. These mathematical components included integrators, adders and XYZ look up tables. The second circuit was driven by two input terminals. The X input which was the temperature and the Y input which was the SOC. Throughout the simulation the X input varied because of the data in the lookup tables and the Y input varied because of the SOC in the first circuit. Once the simulations for all temperatures were completed the average marginal error came to be 2.1% therefore making PSCAD an accurate simulation tool for modeling circuits. Therefore this justifies that PSCAD is a precisemodeling tool. After comparing the measured and simulated plots, the results revealed that PSCAD is a useful resource for depicting the functionality of batteries under constant discharge and numerous temperatures. For future industries, this determines that PSCAD can be used as a sufficient tool to analyze and evaluate the characteristics of batteries for the use of electric vehicle technology.

## **Acknowledgement**

I would like to thank my professor, ZiyadSalameh, whose encouragement, guidance and support from the initial to the final level enabled me to develop and understand the modeling of batteries and their importance to electric vehicles. I am grateful for the assistance of Dipesh Patel and Shiv Sharma in aiding in the completion of this thesis. I would also like to thank Prof. MufeedMah'd and Prof. Joel Therrien for agreeing to serve on my thesis committee. Lastly, I offer my gratitude and blessings to all of my colleagues and family for supporting me in any respect during the completion of this thesis.

## **Table of Contents**

Introduction.....	1
Battery Evaluation Lab at UMass Lowell.....	6
Methodology of constructing a circuit model for a Lithium Iron Phosphate Battery Using PSCAD.....	10
Introduction to PSCAD.....	10
Modeled Circuit.....	11
Finding Open Circuit Voltage ( $V_{oc}$ ).....	14
Finding Internal Resistance ( $R_{dc}$ ) .....	16
Finding R's and C's.....	17
Setting up simulation in PSCAD.....	21
Validation of the model by comparing the simulated and the experimental results.....	25
Discussion .....	35
Conclusion and future work.....	36
References.....	38
Appendix 1.1.....	41
Appendix 1.2.....	42
Appendix 1.3.....	43
Appendix 1.4.....	45
Biography.....	48

## **List of Figures**

Figure 1: Battery tester station with temperature chamber.....	7
Figure 2: Arbin instruments battery and capacitor tester.....	8
Figure 3: The Thevenin equivalent oriented battery model circuit.....	11
Figure 4: The impedance based oriented battery model circuit.....	12
Figure 5: The runtime based oriented battery model circuit.....	12
Figure 6: Designed circuit for battery modeling.....	13
Figure 7: Terminal Voltage vs. Time.....	18
Figure 8: SOC circuit oriented model.....	22
Figure 9: Equivalent PSCAD Circuit.....	23
Figure 10: Terminal voltage equivalent circuit.....	24
Figure 11: Instantaneous SOC vs. Time.....	25
Figure 12: Terminal and simulation voltage at 0 degrees C.....	26
Figure 13: Terminal and simulation voltage at 20 degrees C.....	27
Figure 14: Terminal and simulation voltage at 30 degrees C.....	27
Figure 15: Terminal and simulation voltage at 40 degrees C.....	28
Figure 16: Terminal and simulation voltage at 0 degrees C.....	29
Figure 17: Terminal and simulation voltage at 20 degrees C.....	30
Figure 18: Terminal and simulation voltage at 30 degrees C.....	31
Figure 19: Terminal and simulation voltage at 40 degrees C.....	32
Figure 20: $V_{oc}$ vs. SOC data points and fitting curves at 0 degrees C.....	33
Figure 21: Data points and fitting curves for all four temperatures.....	34

**List of Tables**

Table 1: Major electric vehicle battery comparison.....4

Table 2: Performance comparison between lithium ion cobalt and lithium iron phosphate battery.....6

Table 3:  $R_{dc}$  values for different temperatures.....16

Table 4: Final resistor and capacitor values for different temperatures.....21

Table 5: Marginal temperature for all temperatures.....35

## **List of Equations**

Equation 1.....	14
Equation 2.....	14
Equation 3.....	14
Equation 4.....	15
Equation 5.....	15
Equation 6.....	15
Equation 7.....	15
Equation 8.....	16
Equation 9.....	18
Equation 10.....	19
Equation 11.....	19
Equation 12.....	19
Equation 13.....	20
Equation 14.....	20
Equation 15.....	21
Equation 16.....	22

## **Introduction**

Looking at the 21<sup>st</sup> century, internal combustion engine vehicles (ICEV) are very harmful to humans and the environment. These vehicles produce carbon dioxide (CO<sub>2</sub>), carbon monoxide (CO), sulfur dioxide (SO<sub>2</sub>), and many other harmful toxic gases. In addition to polluting the air these vehicles generate greenhouse effect gases, wasted heat, and they require toxic fuels to operate. Moreover, ICEV's require frequent maintenance and only have a life span of about 100,000 - 200,000 miles. [1] Since ICEV's can be so harmful, the development of electric vehicle technology has increased substantially within the last few decades.

Electric Vehicles (EV) are said to be environmentally friendly and pollution free. Due to the fact that there is only one rotating part, the motor, these vehicles are maintenance free. All the other components, such as the battery and controller, don't require maintenance for a long period of time. Also, EV's do not require toxic gases to operate and are equipped with regenerative braking. This implies that when the brakes are applied or when the car is moving down a hill the motor acts as a generator and supplies energy back to the batteries which in turn charges them. Furthermore, an electric motor has a long life span and can run for millions of miles before it needs to be replaced. [1] Although EV's have a lot of positive advantages over ICEV's they also have flaws. Two of the biggest flaws are the distance traveled on one charge (the range) and the charging time of the batteries used in the EV's.

A fully charged EV with lead acid batteries can travel a distance of approximately 60 miles. [1] An acceptable distance for many commuters, however it's not substantial

enough for individuals that are traveling long distances. A solution to this problem is developing better batteries that have high energy density so that the vehicles are able to travel longer distances. Using a good quality battery ensures that the vehicle will be able to travel longer distances and will make it more efficient. Another issue that requires attention is charging these batteries after they have fully discharged.

When an EV has fully discharged it can take anywhere from 4-8 hours to fully charge a car again. [1] This creates several issues. For one, if every individual was to charge their vehicles around the same time the utility companies would be chaotic because so much power would be used to charge all of the electric vehicles. A solution to this issue is a technology known as vehicle- grid technology (V2G). Another issue is that it only takes about 5-10 minutes to fully fill an ICEV which makes it more appealing. The Society of Automotive Engineers (SAE) is designing several EV battery chargers to provide faster charging for EV. These battery chargers are classified by the level of power they dissipate. The level 1 battery chargers provide the standard voltage and current found in the three prong outlets used in homes: 120 volts AC and 15 amps. The power output from these devices is approximately 1-1.9 kW and can typically take anywhere from 4-8 hours to fully charge a vehicle. The level 2 battery chargers provide a voltage of 240 volts and a current of 40 amps. These chargers have a power output of 2-7.6kW and can take anywhere from 2-2.5 hours to fully charge a vehicle. The level 3 battery chargers are still under development. Researchers are trying to develop a three phase 60 Hz fast charging stations that will deliver 208 volts AC to 600 volts AC to the vehicles. [1] This will provide a 50% charge return to the vehicle in no more than 5

minutes and 80% charge return in no more than 15 minutes. [2] Once this technology has fully developed it will bring a new appeal to EV's.

Due to the nature of electric vehicles, these batteries must be able to withstand various temperatures conditions and fast charging rates. This means that the batteries must be robust, dependable, and stable. Research is being done on a number of batteries to develop one that will be best suited for electric vehicle technology. Several batteries that have been tested throughout the years include: Nickel Cadmium (NiCd), Nickel Metal Hydride (NiMH), Lead Acid, Alkaline, Lithium-ion cobalt, and Lithium-ion polymer. These batteries' characteristics can be found in Table 1.

	NiCd	NiMH	Lead Acid	Li-ion	Li-ion Polymer	Reusable Alkaline
Gravimetric Energy Density (Wh/kg)	45-80	60-120	30-50	110-160	100-130	80 (Initial)
Internal Resistance (includes peripheral circuits) mW	100 to 200 6V pack	200 to 300 6V pack	<100 12V pack	150 to 250 7.2V pack	200 to 300 7.2V pack	200 to 2000 6V pack
Cycle Life (to 80% of initial capacity)	1500	300 to 500	200 to 300	500 to 1000	300 to 500	50 (to 50%)
Fast Charge Time	1 hr typical	2-4 hr	8-16 hr	2-4 hr	2-4 hr	2-3 hr
Overcharge Tolerance	moderate	low	high	very low	low	moderate
Self-discharge / Month (room temperature)	20%	30%	5%	10%	~10%	0,3%
Cell Voltage (nominal)	1.25V	1.25V	2V	3.6V	3.6V	1.5V
Load Current -peak -best result	20C 1C	5C 0.5C or lower	5C 0.2C	>2C 1C or lower	>2C 1C or lower	0.5C 0.2 C or lower
Operating temperature (discharge only)	-40 to 60C	-20 to 60C	-20 to 60C	-20 to 60C	0 to 60C	0 to 65C
Maintenance Requirement	30 to 60 days	60 to 90 days	3 to 6 months	Not req.	Not req.	Not req.
Typical Battery Cost (US\$ reference only)	\$50 (7.2V)	\$60 (7.2V)	\$25 (6V)	\$100 (7.2V)	\$100 (7.2V)	\$5 (9V)

Table 1: Major electric vehicle battery comparison

One of the first battery packs used in electric vehicles was the lead acid battery, however these battery packs were bulky in size, weighed close to 1,000 pounds, and only provided about 16kW/hr. Recent studies have shown that lithium based batteries provide 3 times the energy with half the weight of the lead acid batteries. The lithium based

batteries are also smaller in size (100 microns thick) and deliver a higher nominal voltage (the rated voltage of the battery).

An upcoming battery that is being researched and compared to the lithium-ion battery is the lithium iron phosphate battery. The lithium iron phosphate ( $\text{LiFePO}_4$ ) battery ran through more than 1,000 cycles before its capacity fell to 80%. This is a substantial improvement compared to the lithium-ion battery. The lithium-ion cobalt battery fell to 80% capacitance after 50 cycles. [3] More tests and comparisons were performed on both these batteries and it was seen that by comparison the lithium iron phosphate battery was more suitable for electric vehicles. Some notable characteristics about the  $\text{LiFePO}_4$  battery compared to the lithium ion cobalt battery were that there was a lower safety risk, a higher specific energy density, it was cheaper, and it was more environmentally friendly. The full comparison between the two batteries can be seen in Table 2.

	LiCoO <sub>2</sub>	LiFePO <sub>4</sub>
Operating Temperature	-20 to 60 C	-10 to 60 C
Maximum DoD	20%	5%
Life (years)	2-3	Unknown
Life (cycles)	3000	1000 to 3000
Nominal Voltage	3.7	3.2
Memory Effect	No	No
Safety Risk	Nominal	VeryLow
Theoretical Specific Energy Density	602 W-h/kg	549 W-h/kg
Specific Energy Density	140 -155 W-h/kg	130-170 W-h/kg
Volumetric Energy Density	3073 W-h/L	1976 W-h/L
Material Cost	Higher	Lower
Environmentally Friendly	Lower	Higher

Table 2: Performance comparison between lithium ion cobalt and lithium iron phosphate battery

### Battery Evaluation Lab at UMass Lowell

Since the 1990's, there has been a battery evaluation lab at the University of Massachusetts Lowell (UML). This lab was designed to evaluate various types of batteries and their suitability for use in electric vehicles. [4] The lab has three independent battery exerciser and data recording systems. These systems are designed to test batteries that range from 0.1 mV to 20 volts at 0.1mA to 320amps. [2] Each system

controls different types of current regulators that are suitable for various kinds of batteries. The batteries can be charged or discharged due to the fact that the regulators can source or sink different currents. [4] In addition to the current regulators, there are two computer controlled environmental chambers that provide the batteries with the preferred ambient temperatures. [2] Due to the nature of the environmental chamber, a precise analysis on the battery can be achieved to replicate the performance of the battery in an electric vehicle. Figure 1 shows an image of the battery testing station with the temperature chamber.

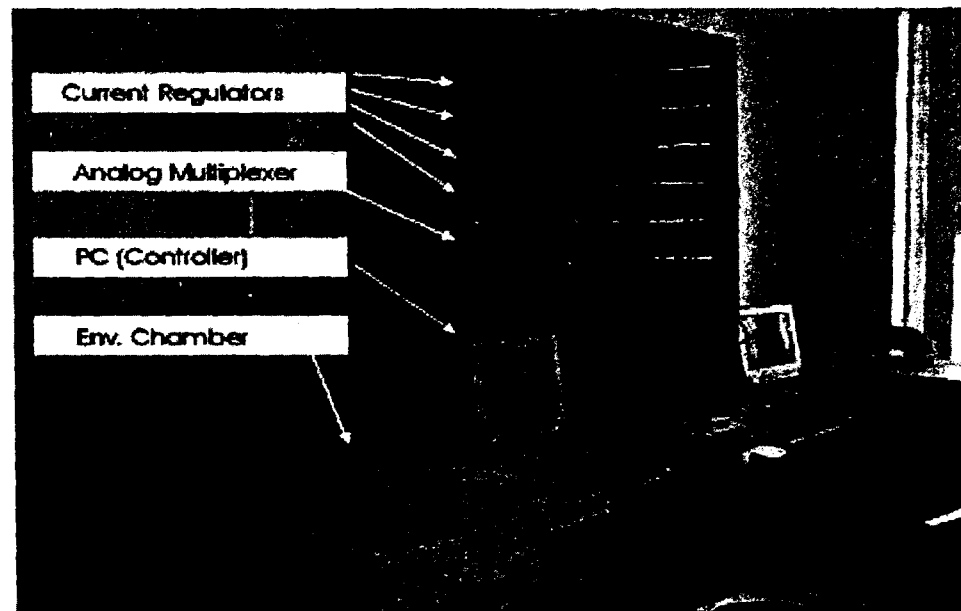


Figure 1: Battery tester station with temperature chamber

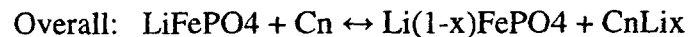
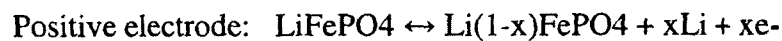
Another battery testing station that is available at UMass Lowell is the Arbin instruments battery and capacitor tester. This tester can test voltages that range from 0 to 60 volts. It can also charge test charging and discharging currents from 0 to 100 amps. This system can collect and record data during the test cycle. This system provides a user friendly function that allows for easily drawing output graphs from saved excel files. This

tester has a fast response time ( a few milliseconds) which allows for it to change from charge to discharge relatively quickly. The image of this system is shown in Figure 2.



Figure 2: Arbin instruments battery and capacitor tester

This thesis models only the discharging battery characteristics of a 160Ah lithium iron phosphate battery under various ambient temperatures (0C, 20C, 30C, and 40C). The lithium iron phosphate battery uses lithium iron phosphate as the positive electrode and a highly crystallized specialty carbon as the negative electrode. Both the reactions at the electrodes are regulated by a liquid electrolyte lithium hexafluorophosphate ( $\text{LiPF}_6$ ) and organic solvents. [4] The chemical reaction for this battery is as follows:



The nominal terminal voltage for this battery is 3.3 volts which results in a 528Wh energy rating. The  $\text{LiFePO}_4$  battery is a prismatic cell in a plastic case measuring at 27.5 x 18.3 x 7.1 cm for a volume of 3,674 cubic centimeters. This produces a volumetric

energy density of 143 Wh/L. This cell weighs approximately 5.2kg which yields in a gravimetric energy density of 101.5 Wh/kg. [4]

The charging characteristics could not be modeled due to insufficient data collection. When fully charging the battery, the nominal voltage was not reaching its full potential of 3.3 volts. It was only reaching a nominal voltage of 3 volts. This would provide inadequate data for modeling purposes. Additionally when the data for the battery was collected, the transient data was not observed which resulted in no data collection for the open circuit voltage at different state of charges. Therefore the modeling of the full discharge was fairly inaccurate. Since the transient data was not collected, only partial data was used to model the discharging characteristics of the battery. The methods used to model this battery are explained later in this paper.

In order to model batteries an accurate equivalent circuit must be constructed. There are various types of modeling methods. Some of these include physical, empirical abstract, mixed, and electrical circuit models. For this thesis, a linear electrical circuit model was used based on fixed parameters given a varying state of charge (SOC). Using PSCAD, circuits were constructed using linear passive elements, voltage sources and look up tables to model the characteristics. Capacity fading was modeled using a capacitor whose capacitance decreases linearly with the number of cycles. The voltage across this capacitance represents the ratio of delivered capacity to full charge capacity. The temperature effect was modeled using a resistor-capacitor circuit with two temperature dependent sources. [5]

## **Methodology of constructing a circuit model for a Lithium Iron Phosphate Battery Using PSCAD**

### **Introduction to PSCAD:**

Power systems computer aided design also known as PSCAD is a quick, accurate, and user friendly simulation software for all different types of power system designs. Its graphical user interface helps improve the control and usability of the simulation environment. This software allows its users to efficiently construct a circuit and run a simulation. Once the simulation is complete the data and results can be analyzed in a completely graphical environment. Many companies have adopted PSCAD for its dependability, accuracy, and broad library of power and control system models. [6]

PSCAD uses Electromagnetic Transients including DC (EMTDC) as the essential part of the graphical user interface. EMTDC is used to solve differential equations in the time domain. Due to its program structure, control systems can be represented with or without electromechanical or electromagnetic systems existing. [7]

PSCAD has an extensive library that ranges from simple passive elements or control functions to electric machines and transmission lines. Due to this complete library users can construct several advanced nonlinear models into one large model. [8] For this thesis PSCAD is being used to model the runtime based circuit of a discharging Lithium Iron Phosphate battery under various temperatures.

### Modeled Circuit:

It is difficult to account for the change in battery parameters under different states of charges and conditions. Circuit based battery models use a combination of various resistors, capacitors, and voltage and current sources to model the performance of a battery. There are three basic forms of electrical models. These models include a Thevenin, impedance based, and runtime based equivalent circuit. The circuit used to evaluate this thesis was the runtime based equivalent circuit. [9]

The most simplistic form of modeling a battery is the Thevenin equivalent circuit. This circuit is shown in Figure 3. It consists of a voltage source ( $V_{oc}(SOC)$ ) that is a function of state of charge (SOC) in series with the batteries internal resistance ( $R_o$ ) and the parallel resistor-capacitor (R-C) combinations. The R-C combinations predict the response to a transient load at specific SOC's by assuming that the open circuit voltage ( $V_{oc}$ ) is constant. Therefore, this model is unable to reflect the influence of the SOC to the battery behavior properly. [9]

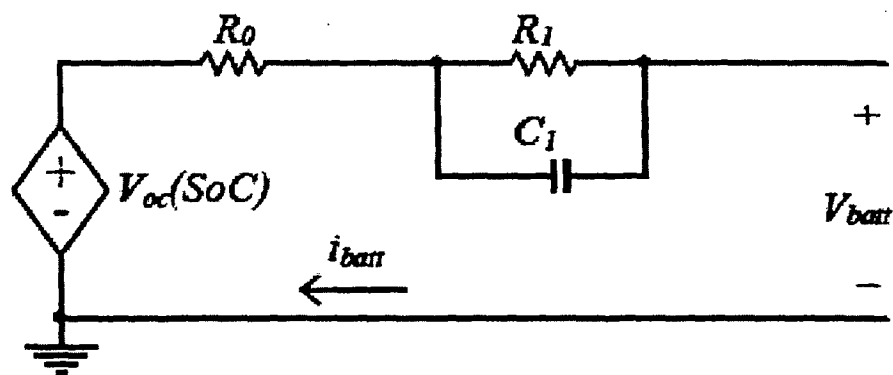


Figure 3: The Thevenin equivalent oriented battery model circuit.

An impedance based circuit is shown in Figure 4. This circuit acquires an AC-equivalent impedance model in the frequency domain. It then uses a complex equivalent system ( $Z_{ac}$ ) to fit the impedance ranges. This fitting process is very difficult and complex. Additionally, since these models only work for fixed SOC's and temperatures, they cannot predict battery runtime or DC response. [9]

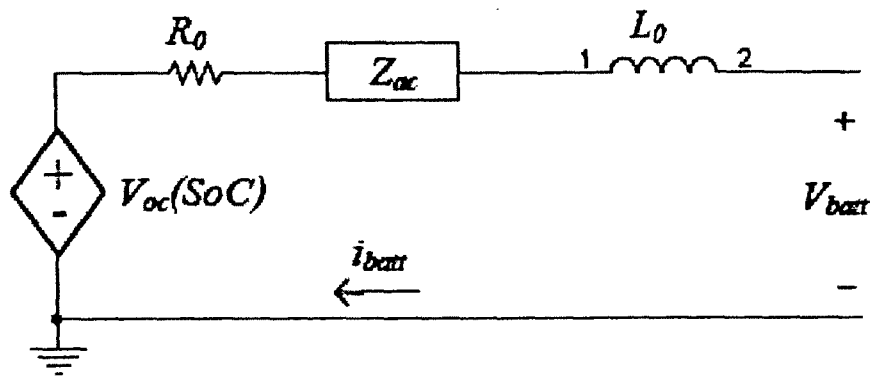


Figure 4: The impedance based oriented battery model circuit.

Runtime based models, shown in Figure 5, use complex circuits to simulate the DC voltage response and runtime of the battery. This model uses two different circuits to depict the battery characteristics.

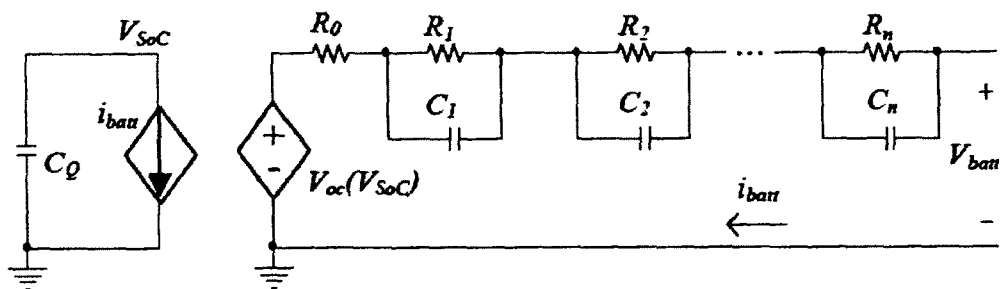


Figure 5: The runtime based oriented battery model circuit

The circuit located to the left of Figure 5 depicts a capacitor ( $C_Q$ ), which contains the value of the battery capacitance, and a dependent current source which represents the

batteries state of charge. The R-C networks, on the right side of the circuit, represent the relationship between the battery current and terminal voltage. This circuit is similar to the Thevenin's equivalent circuit.

For this thesis a runtime based model was chosen using 3 R-C network connections. The 3 R-C networks were selected because when using 2 networks the simulation results were not matching the experimental data. Also, the difference in plots for the experimental and measured data was negligible when using more than 3 R-C networks. Figure 6 shows the final design used to replicate the battery characteristics.

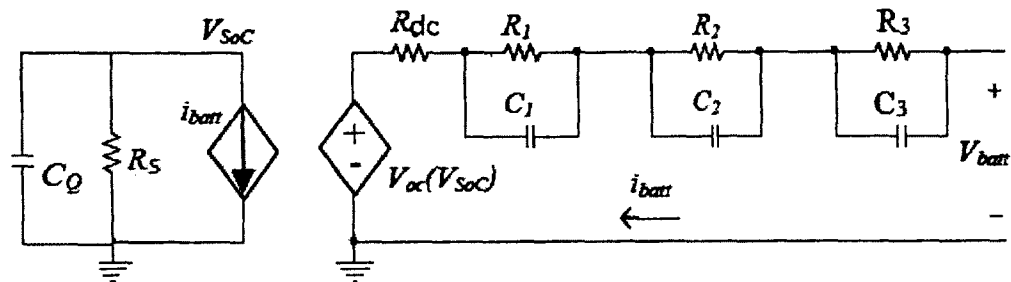


Figure 6: Designed circuit for battery modeling

The first circuit is a dependent current source that is in series with a resistance. This portion of the circuit shows how the batteries SOC will vary with the batteries current. The second circuit is an R-C circuit that is equivalent to the Thevenin circuit. This section of the circuit represents the relationship between the battery current and the terminal voltage. [9]

The internal resistance ( $R_s$ ) multiplied by the current in the battery ( $I_b$ ) represents the internal resistance voltage loss. Looking at Figure 6, it is observed that  $V_{soc}$  simulates the batteries SOC, and also that the voltage dependent source  $V_{oc}(S_{oc})$  is a function of this SOC. When looking at the mathematical equation, Equation 1, it can be

seen that the voltage  $V_i$  can be construed as the voltage drop of the low-pass filter battery current over the resistor  $R_i$  of the R-C system. [9]

$$V_i(s) = R_i * \frac{\frac{1}{R_i * C_i}}{s + \frac{1}{R_i * C_i}} \quad (1)$$

The cutoff frequency of the low-pass filter is:

$$F_{cutoff} = \frac{1}{R_i * C_i} \quad (2)$$

Based on this mathematical model, the combined effect of all the R-C systems, in the runtime based model, is equivalent to a subsequent low-pass filter applied to an ensuing R-C system resistance. It should be noted that when deriving the mathematical models the values of  $R_i$  and  $C_i$  were determined as a function of SOC. This means that when creating an equivalent circuit the values of resistors and capacitors must also be a function of SOC.[9]

#### **Finding Open Circuit Voltage (Voc):**

The open circuit voltage (Voc) at each SOC was to be determined because no transient data was provided. Equation 3 was used to find Voc at each SOC.

$$V_{oc} = V_t + I_{dis} * R_{dc} \quad (3)$$

In Equation 4,  $V_t$  is the terminal voltage at each specific SOC (i.e. SOC=1, SOC =0.9, SOC =0.8....etc). The constant discharge current,  $I_{dis}$ , is 80 Amps, and  $R_{dc}$  is the internal resistance for the respective temperature. The tabular data for the estimated transient  $V_{oc}$  for each specific SOC and temperature can be found in Appendix 1.1. Using the experimental data, a graph of  $V_{oc}$  vs. SOC for each individual temperature was then plotted using MATLAB. An equation for  $V_{oc}$  was developed by fitting the best fit curve to the graph of  $V_{oc}$  vs SOC. Equations 4-7 show  $V_{oc}$  as a function of SOC for their respected temperatures.

$$V_{oc0} = (312.37 * SOC^7) - (1263.2 * SOC^6) + (2133.8 * SOC^5) - (1950.7 * SOC^4) + (1043.6 * SOC^3) - (328.16 * SOC^2) + (56.91 * SOC) - 0.69614(4)$$

$$V_{oc20} = (209.38 * SOC^7) - (730.76 * SOC^6) + (1033.6 * SOC^5) - (760.03 * SOC^4) + (310.05 * SOC^3) - (69.525 * SOC^2) + (8.2053 * SOC) + 3.0066(5)$$

$$V_{oc30} = (364.93 * SOC^7) - (1310.4 * SOC^6) + (1913.7 * SOC^5) - (1459.3 * SOC^4) + (620.21 * SOC^3) - (145.19 * SOC^2) + (17.425 * SOC) + 2.5669(6)$$

$$V_{oc40} = (206.21 * SOC^7) - (707.4 * SOC^6) + (969.27 * SOC^5) - (672.31 * SOC^4) + (245.26 * SOC^3) - (43.517 * SOC^2) + (2.9525 * SOC) + 3.515(7)$$

Once these equations were found, a varying SOC from 0 to 1 in 0.001 increments was plugged back into the equation using MATLAB in order to find all the data points for  $V_{oc}$ . These values were placed into tables that were used as look up tables in PSCAD. Due to the extensive data for these look up tables, the tabular data is not provided.

### Finding Internal Resistance ( $R_{dc}$ )

To begin finding a resistance value for the internal resistance,  $R_{dc}$ , the discharging data for all four temperatures was sorted out. Once the data was sorted out the nominal voltage ( $V_t$ ) was found for each temperature. After finding the nominal voltage, the first voltage drop ( $V_{d1}$ ) was obtained by using the voltage at which the current became stable. The constant discharge current ( $I_{dis}$ ) was set to 80 amps. Once all these parameters were determined, Equation 8 was used to determine  $R_{dc}$ .

$$R_{dc} = \frac{V_t - V_{d1}}{I_{dis}} \quad (8)$$

Table 3 shows all the  $R_{dc}$ 's for their respected temperatures. This data showed that as the temperature hit extreme high and low values (0C and 40C) the  $R_{dc}$  values were at their highest points (6.599m $\Omega$  and 5.419m $\Omega$  respectively).

Temperature (degrees C)	Rdc( $\Omega$ )
0	0.006599
20	0.0045375
30	0.004161
40	0.005419

Table 3:  $R_{dc}$  values for different temperatures

### Finding R's and C's:

When creating an equivalent circuit, the number of parallel R-C networks must be determined. Research has shown that the number of parallel R-C combinations that should be in series with  $R_{dc}$  are between 2 and 3. Anything less than 2 combinations will predict inaccurate data and anything more than 3 combinations will make negligible changes to the output of the simulation. [10] As mentioned before, 3 parallel R-C networks were used because when 2 networks were used the simulation results were not matching the experimental data.

A series of equations must be used in order to calculate the resistor and capacitor values of an R-C network. There are various data points that need to be determined before beginning these calculations. In order to obtain the correct data the terminal voltage vs. time chart is first plotted. Once this has been complete, the values of the variables  $V_{d1}$ ,  $V_{d2}$ ,  $V_{d3}$ ,  $V_{d4}$ ,  $\tau_1$ ,  $\tau_2$ ,  $\tau_3$ , and  $\tau_4$  can be determined. These values will be used in their respective equations to determine  $R_1$ ,  $R_2$ ,  $R_3$ ,  $R_4$ ,  $C_1$ ,  $C_2$ , and  $C_4$ . Figure 7 shows how these values can be determined.

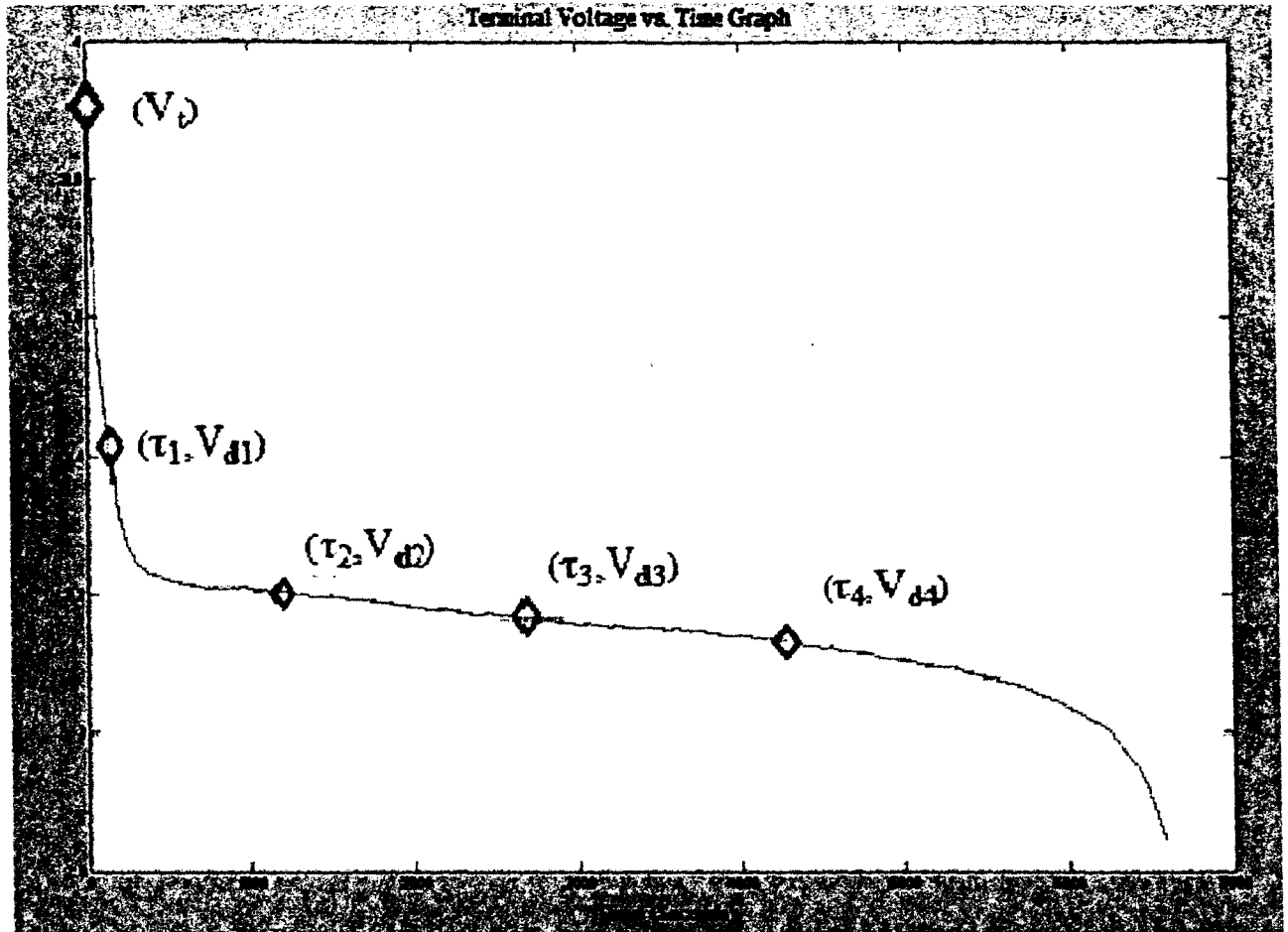


Figure 7: Terminal Voltage vs. Time

Resistor  $R_1$  is known as a short time constant resistor. Since the battery is constantly discharging with time,  $R_1$  depicts the resistance over a short period of time after the battery has discharged through the internal resistance  $R_{dc}$ . Equation 9 shows the equation used to determine  $R_1$ .

$$R_1 = \frac{V_{d1} - V_{d2}}{I_{dis}} \quad (9)$$

In this equation  $V_{d1}$  is the voltage drop right after the internal resistance and it occurs at a specific time  $(\tau_1)$ .  $V_{d2}$  is the voltage drop that occurs after a short time interval  $(\tau_2)$ . The constant discharge current is denoted as  $I_{dis}$ .

After defining the value for  $R_1$ , the capacitance  $C_1$  had to be determined. Equation 10 shows how  $C_1$  was calculated.

$$C_1 = \frac{\tau_2 - \tau_1}{R_1} \quad (10)$$

In this equation,  $\tau_2$  is the time at which  $V_{d2}$  was determined, and  $\tau_1$  is the time at which  $V_{d1}$  occurred.  $R_1$  is the value calculated using Equation 9.

Resistor  $R_2$  is known as the medium time constant branch resistor.  $R_2$  depicts the resistance over a time period that can be equal to or greater than the time interval of  $R_1$  but less than or equal to the time interval of  $R_3$ . Equation 11 shows the equation for calculating  $R_2$ .

$$R_2 = \frac{V_{d2} - V_{d3}}{I_{dis}} \quad (11)$$

In this equation  $V_{d2}$  is the voltage drop right after  $R_1$  and it occurs at a specific time ( $\tau_2$ ).  $V_{d3}$  is the voltage drop that occurs after a medium time interval ( $\tau_3$ ). The constant discharge current is denoted as  $I_{dis}$ .

After defining the value for  $R_2$ , the capacitance  $C_2$  had to be determined. Equation 11 shows how  $C_2$  was calculated.

$$C_2 = \frac{\tau_3 - \tau_2}{R_2} \quad (12)$$

In this equation,  $\tau_3$  is the time at which  $V_{d3}$  was determined, and  $\tau_2$  is the time at which  $V_{d2}$  occurred.  $R_2$  is the value calculated using Equation 11.

Resistor  $R_3$  is known as the long time constant resistor.  $R_3$  depicts the resistance over a time period that can be equal to or greater than the time interval of  $R_2$ . Equation 13 shows the equation for calculating  $R_3$ .

$$R_3 = \frac{V_{d3} - V_{d4}}{I_{dis}} \quad (13)$$

In this equation  $V_{d3}$  is the voltage drop right after  $R_2$  and it occurs at a specific time ( $\tau_3$ ).  $V_{d4}$  is the voltage drop that occurs after a long time interval ( $\tau_4$ ). The constant discharge current is denoted as  $I_{dis}$ .

After defining the value for  $R_3$ , the capacitance  $C_3$  had to be determined. Equation 14 shows how  $C_3$  was calculated.

$$C_3 = \frac{\tau_4 - \tau_3}{R_3} \quad (14)$$

In this equation,  $\tau_4$  is the time at which  $V_{d4}$  was determined, and  $\tau_3$  is the time at which  $V_{d3}$  occurred.  $R_3$  is the value calculated using Equation 13.

Table 4 shows the values of all the resistors and capacitors used for the R-C parallel networks for each temperature.

Temperature (Degrees C)	R <sub>1</sub> (Ω)	C <sub>1</sub> (F)	R <sub>2</sub> (Ω)	C <sub>2</sub> (F)	R <sub>3</sub> (Ω)	C <sub>3</sub> (F)
0	0.00136	44117.65	0.0007375	162711.86	0.000425	988235.29
20	0.00305	39344.26	0.00925	129729.73	0.0003375	711111.11
30	0.0031375	38247.01	0.0013	92307.69	0.000525	571428.57
40	0.002325	51612.9	0.001275	94117.65	0.00055	654545.45

Table 4: Final resistor and capacitor values for different temperatures

### Setting up simulation in PSCAD:

Once the values of all the components in the circuit ( $V_{oc}$ ,  $R_{dc}$ ,  $R_1$ ,  $C_1$ ,  $R_2$ ,  $C_2$ ,  $R_3$ ,  $C_3$ ) were determined it was time to simulate the circuit using PSCAD. As mentioned before, two circuits were implemented in this modeling to show constant discharge for different temperature. The first circuit consisted of a dependent current source in series with a resistor,  $R_s$ . To begin creating the circuit that is implemented into the dependent current source the following equation must be evaluated.

$$SOC = \frac{\int_0^t I_b dt}{C_b} \quad (15)$$

This equation states that the SOC is equal to the integral of the current with respect to time divided by the capacity of the entire battery. Knowing this equation, the circuit shown in Figure 8 was implemented into PSCAD. The value of resistor  $R_s$  was selected to provide a SOC from 0 to 1.

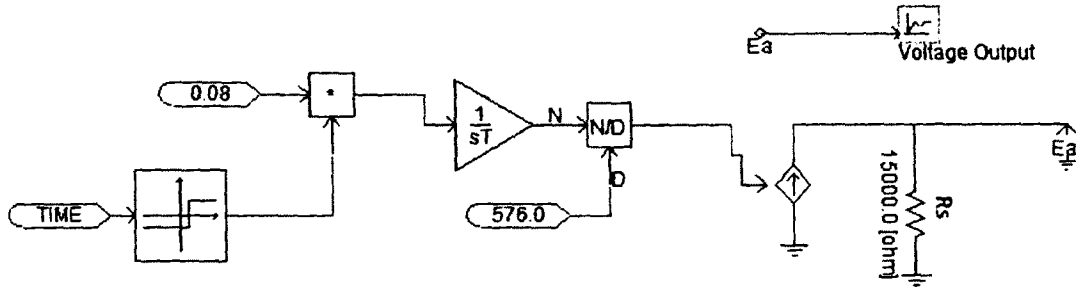


Figure 8: SOC circuit oriented model

After the first circuit was outputting the correct graph the next step was to develop the second circuit. As mentioned above, this circuit consisted of the dependent voltage source in series with  $R_{dc}$  and three parallel R-C networks. The values of all of these components are illustrated using look up tables. The values placed in the look up tables were found using MATLAB and the process of finding these values is explained above. All of these components are dependent on the SOC and temperature of the battery. The lookup table values can be found in Appendix 1.2. Equation 16 shows how the terminal voltage is calculated.

$$V_t = V_{oc} - (I_{dis} * R_{dc}) - [I_{dis} * R_1 * (1 - e^{\frac{-t}{R_1 * C_1}})] - [I_{dis} * R_2 * (1 - e^{\frac{-t}{R_2 * C_2}})] - [I_{dis} * R_3 * (1 - e^{\frac{-t}{R_3 * C_3}})] \quad (16)$$

Figure 9 shows the image of the equivalent circuit using PSCAD.

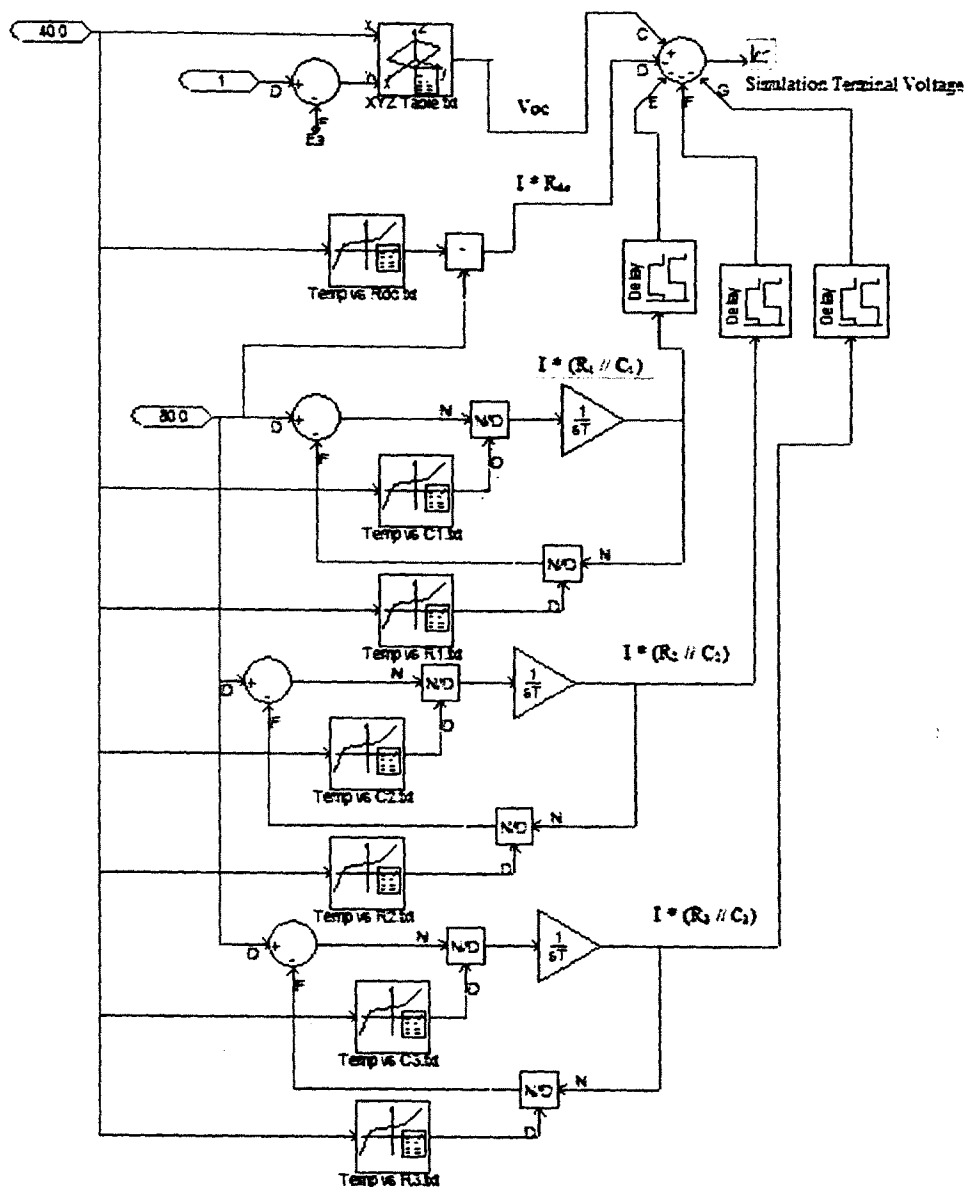


Figure 9: Equivalent PSCAD Circuit

It can be seen that for all the components, the X input is the temperature and the Y input is the SOC. Using these two inputs the look up tables are able to plot the terminal voltage with respect to time. Figure 10 shows the terminal voltage equivalent circuit.

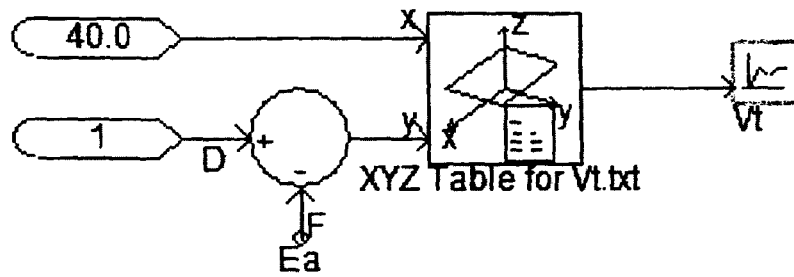


Figure 10: Terminal voltage equivalent circuit

The X input of Figure 10 is the temperature and the Y input is the SOC of the battery. It should also be noted that Figure 9 and Figure 10 can be combined into one circuit by taking the X input of Figure 10 and connecting it to the temperature input in Figure 9.

## Validation of the model by comparing the simulated and the experimental results

Given the simulated circuit in the methodology section the following results were obtained using PSCAD. For the circuit shown in Figure 8 the following graph was developed using PSCAD.

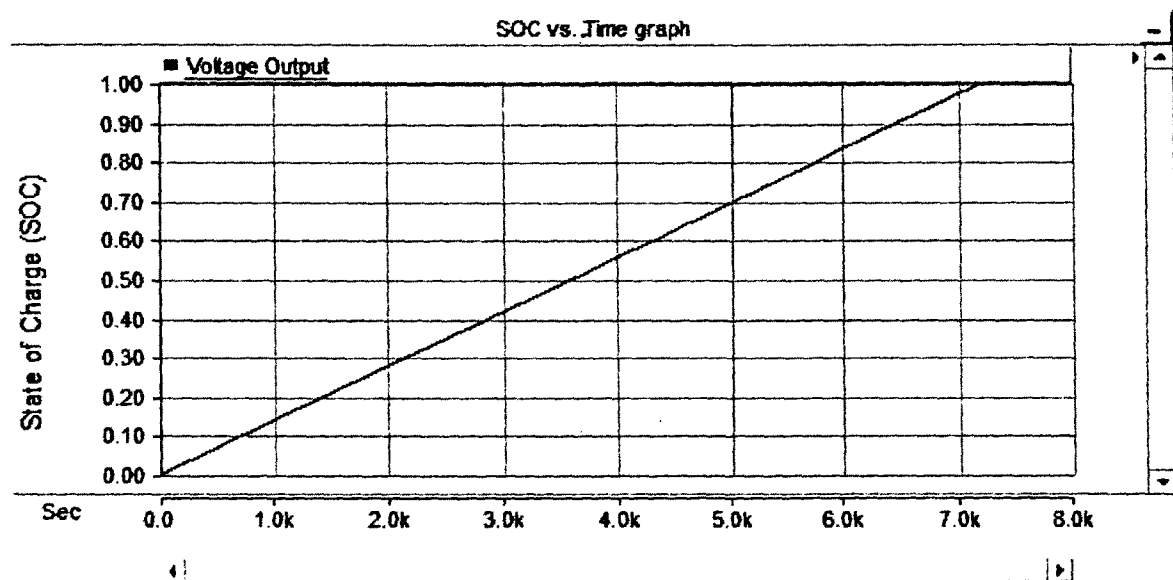


Figure 11: Instantaneous SOC vs. Time

As mentioned before this graph depicts the instantaneous SOC of the battery throughout the entire time it takes the battery to charge and discharge. The Y- axis represents the SOC and it varies from 0 to 1. The X- axis is the time (in seconds) it takes the battery to charge or discharge. The battery took approximately 7200 seconds (2 hours) to charge and discharge because it was a 160Ah Lithium Iron Phosphate battery that was being charged and discharged with a constant 80 amps.

Using the combination of Figures 9 and 10, both the terminal and simulation voltages were plotted and analyzed for each temperature. Figure 12 depicts the plot of terminal vs. simulation voltage for 0 degrees C.

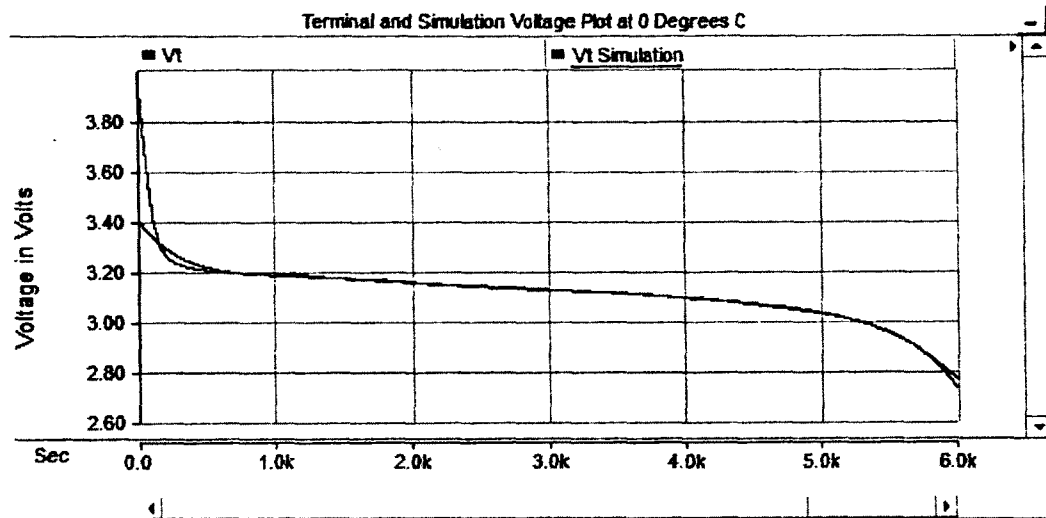


Figure 12: Terminal and simulation voltage at 0 degrees C

It can be seen that the terminal and simulated plots match up fairly well. There are some discrepancies at the beginning of the graph; however those differences exist because the open circuit voltages were estimated, due to the fact that the transient data was not provided for this battery. Also, the data was recorded during long time intervals (60 seconds) which made the data less accurate than a battery that was observed over a shorter time interval (5 seconds). The maximum error for this curve was approximately 3.8%. Figure 13 portrays the plot of terminal vs. simulation voltage for 20 degrees C.

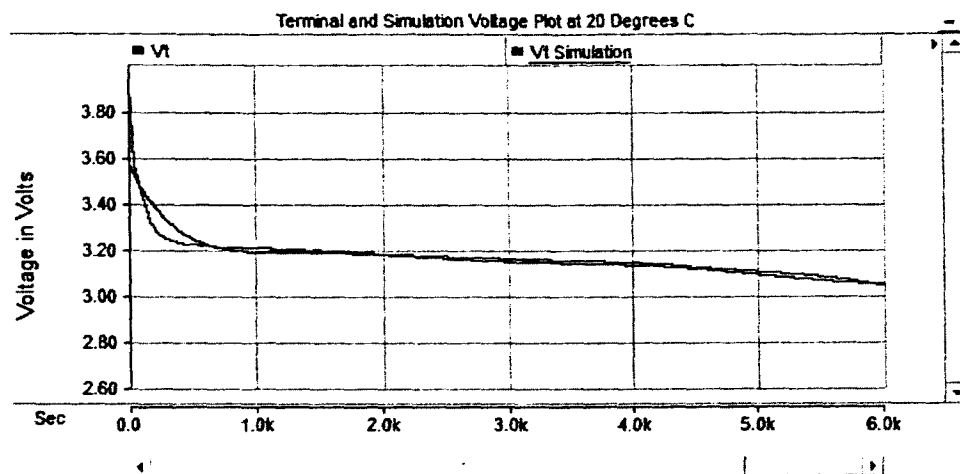


Figure 13: Terminal and simulation voltage at 20 degrees C

Again, it can be seen that the terminal and simulated plots match up fairly well. There are similar discrepancies between the voltage outputs in Figure 12 and 13. The maximum error of the two curves at 20 degrees C was approximately 2.3%. Figure 14 portrays the plot of terminal vs. simulation voltage for 30 degrees C.

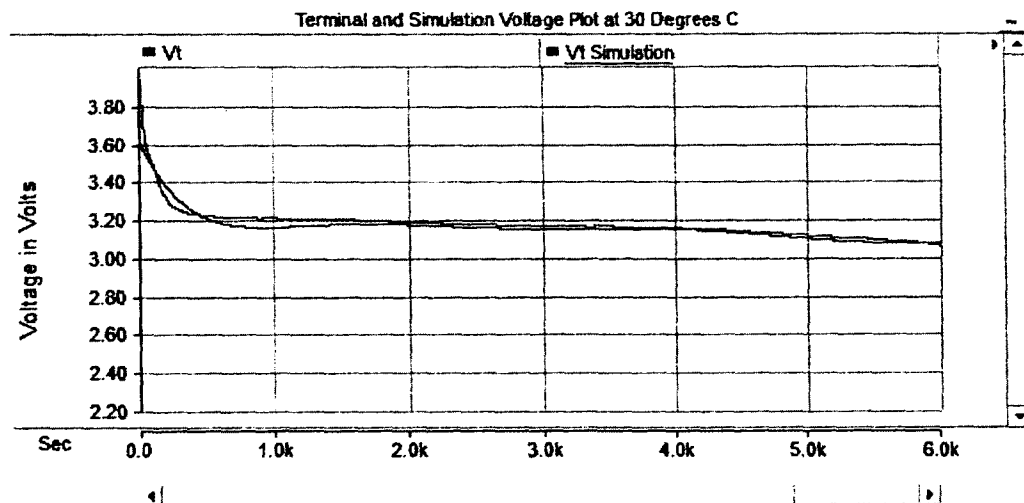


Figure 14: Terminal and simulation voltage at 30 degrees C

Similar to Figure 12 and 13, it can be seen that the terminal and simulated plots match up exceptionally well. There are discrepancies found at the beginning and midpoint of the graph. These differences exist because the open circuit voltages were

estimated, due to the fact that the transient data was not provided for this battery. Also, the data was monitored over a large period of time (60 seconds) which made the data less accurate than a battery that was monitored over a short period of time (5 seconds). The maximum error for these two graphs was approximately 1.25%. Figure 15 portrays the plot of terminal vs. simulation voltage for 40 degrees C.

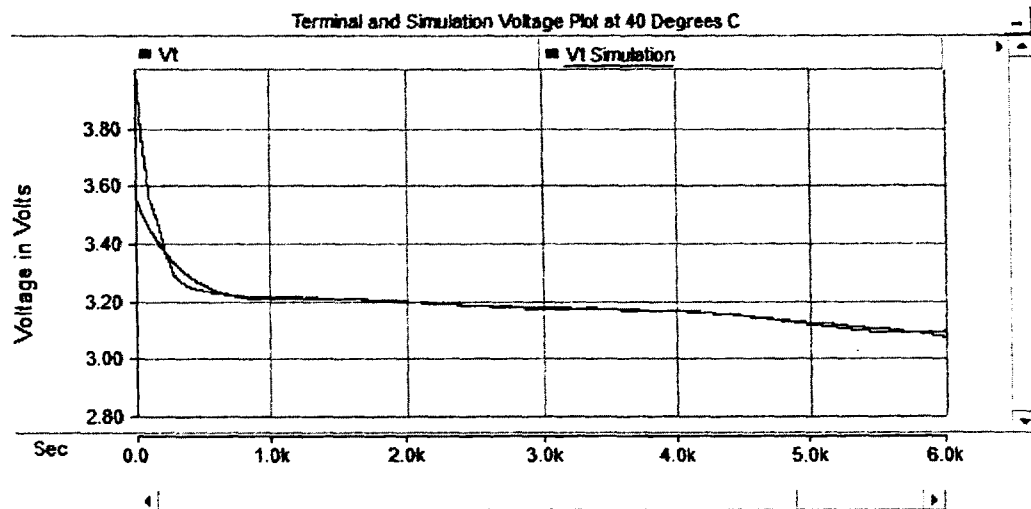


Figure 15: Terminal and simulation voltage at 40 degrees C

Comparably, it can be seen that the terminal and simulated plots match up relatively well. Similar to Figures 12-14, there are some discrepancies at the beginning of the graph; however because no transient data was provided the open circuit voltages were estimated which led to these discrepancies. Also the time in which the data was collected was fairly large (60 seconds) and this can also be a reason for the differences in graphs. The maximum error margin for these two plots was approximately 1.05%.

Overall, all the graphs match up well enough to justify that PSCAD is an accurate and reliable power system simulator. There were a few minor discrepancies between the

collected data and the simulated data; however these differences only occurred because transient data was not collected.

After justifying that the PSCAD simulation was accurate, MATLAB was also used in order to justify the results. Using the MATLAB code in Appendix 1.3, a simulated terminal voltage graph was created using the resistor and capacitor values for their respective temperatures. The simulated graph was then compared to the measured terminal voltage graph. Figure 16 shows the simulated and measured terminal voltages as 0 degrees C.

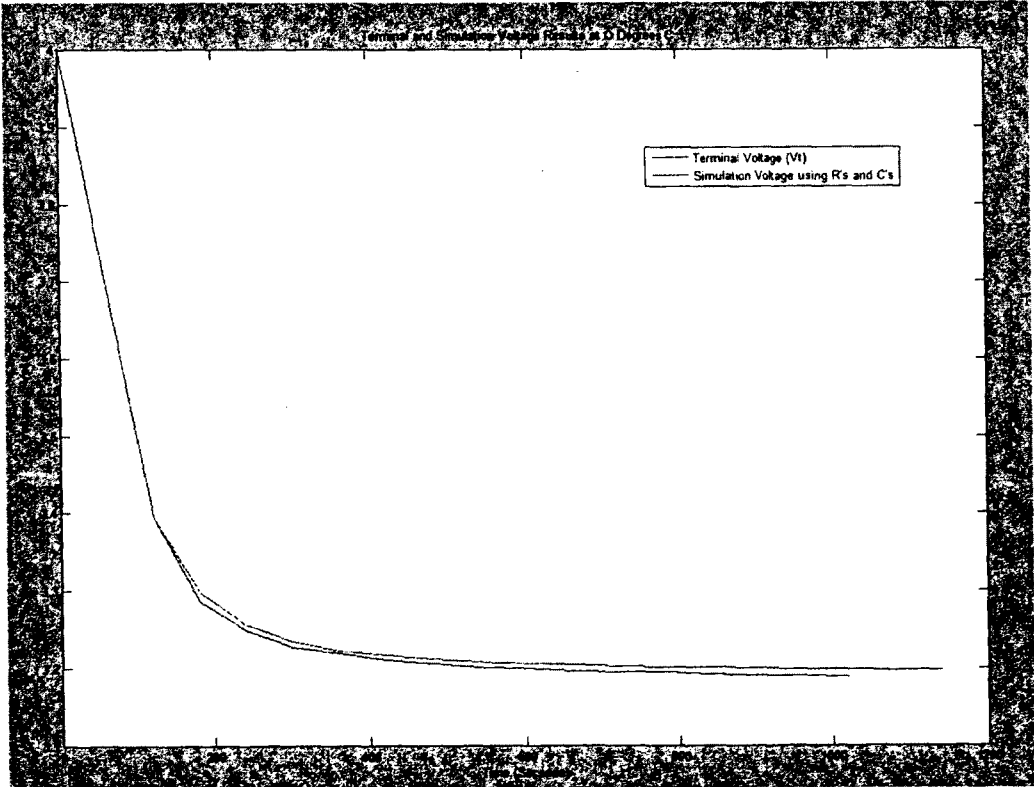


Figure 16: Terminal and simulation voltage at 0 degrees C

Looking at Figure 16, it can be seen that both the simulated and measured terminal voltages are fairly similar. The minor discrepancy between the graphs is due to

the fact that there was no transient data resulting in estimated  $V_{oc}$ 's. Figure 17 shows the simulated and measured terminal voltages as 20 degrees C.

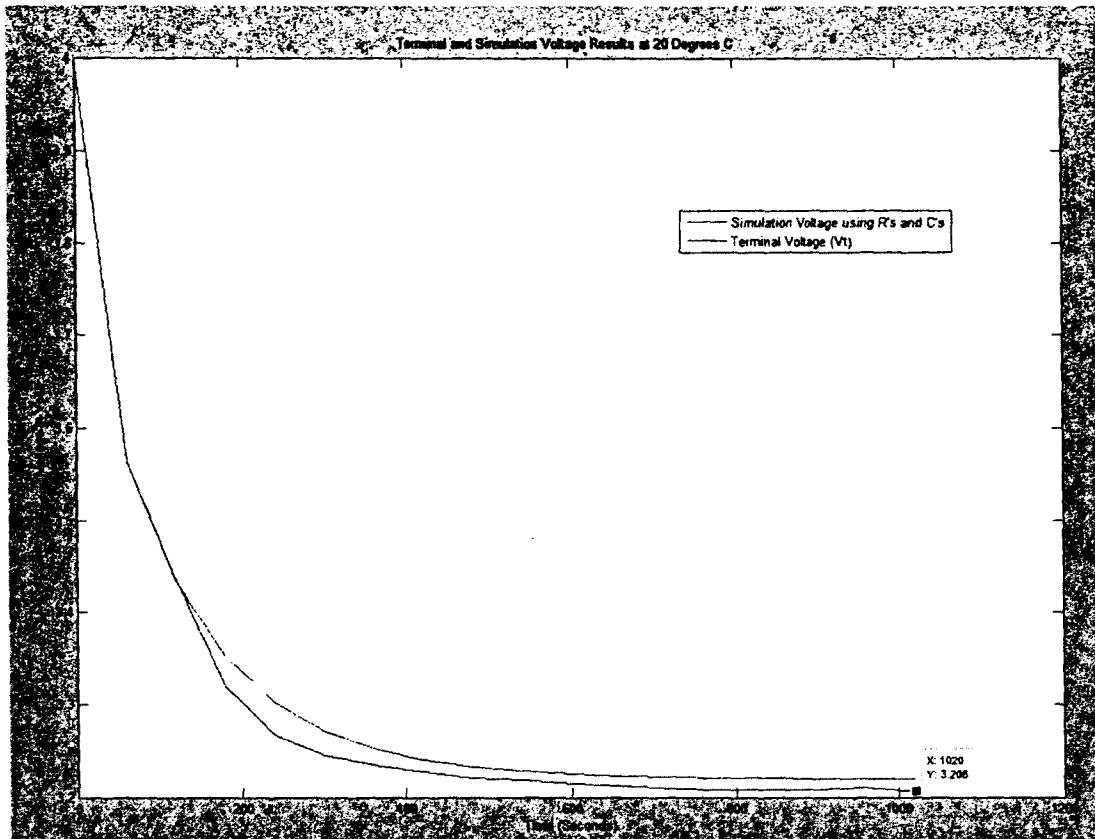


Figure 17: Terminal and simulation voltage at 20 degrees C

Again, Figure 17 shows that both the simulated and measured terminal voltages are fairly similar. The minor discrepancy between the graphs is due to the fact that there was no transient data resulting in estimated  $V_{oc}$ 's, and because the time intervals, at which the data was collected, were very far apart. Figure 18 shows the simulated and measured terminal voltages as 30 degrees C.

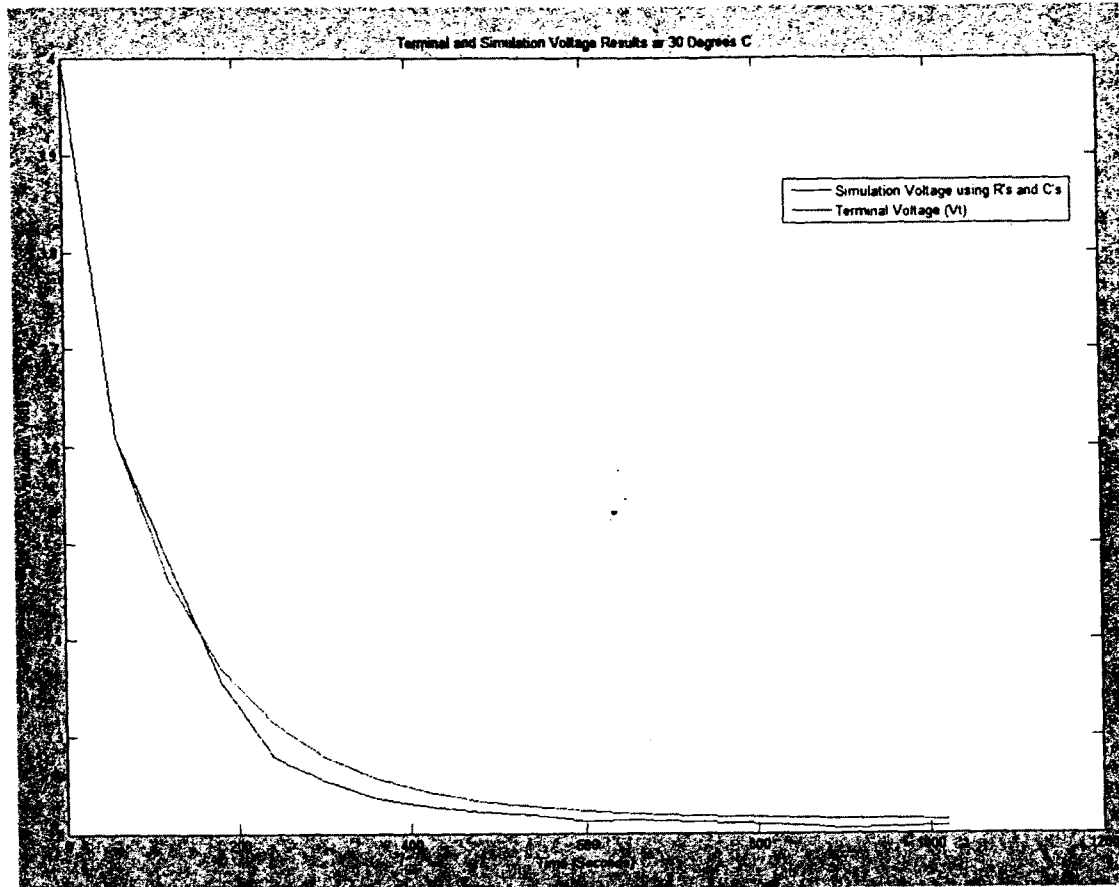


Figure 18: Terminal and simulation voltage at 30 degrees C

Similar to Figure 17, Figure 18 depicts that both the simulated and measured terminal voltages are fairly similar. The minor discrepancy between the graphs is due to the fact that there was no transient data resulting in estimated  $V_{oc}$ 's, and because the time intervals, at which the data was collected, were very far apart. Figure 19 shows the simulated and measured terminal voltages as 40 degrees C.

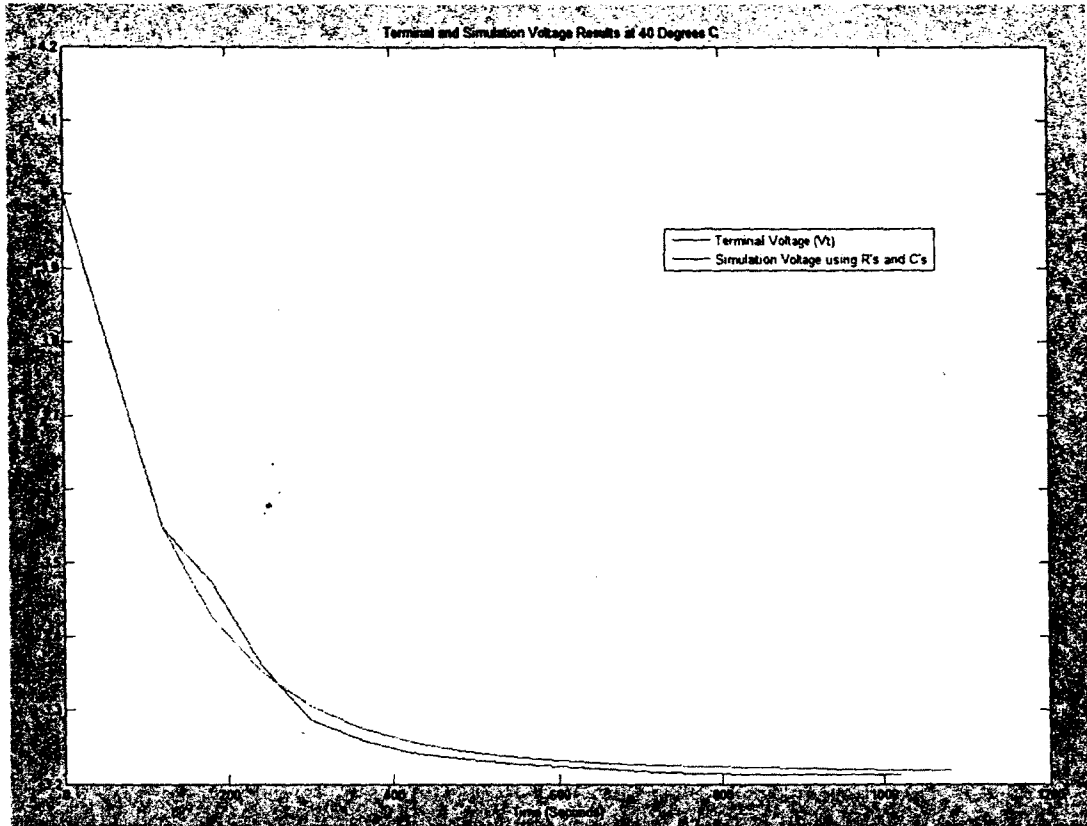


Figure 19: Terminal and simulation voltage at 40 degrees C

Like Figures 16-18, Figure 19 portrays that both the simulated and measured terminal voltages are fairly similar. This graph seemed to have the most discrepancy between the measured and simulated voltages. It seemed as if the measured data points for  $V_t$  were a bit inaccurate. Another reason for the difference between the graphs is that there was no transient data resulting in estimated  $V_{oc}$ 's, and because the time intervals, at which the data was collected, were very far apart.

After comparing all the R-C network curves for the different temperatures, the equation for the open source voltage,  $V_{oc}$ , had to be determined. This was done by plotting the experimental data for  $V_{oc}$  vs. SOC and finding a best fit curve to provide the equation for  $V_{oc}$  at its respected temperature. Figure 20 shows the graph for  $V_{oc}$  vs. SOC at 0 degrees C.

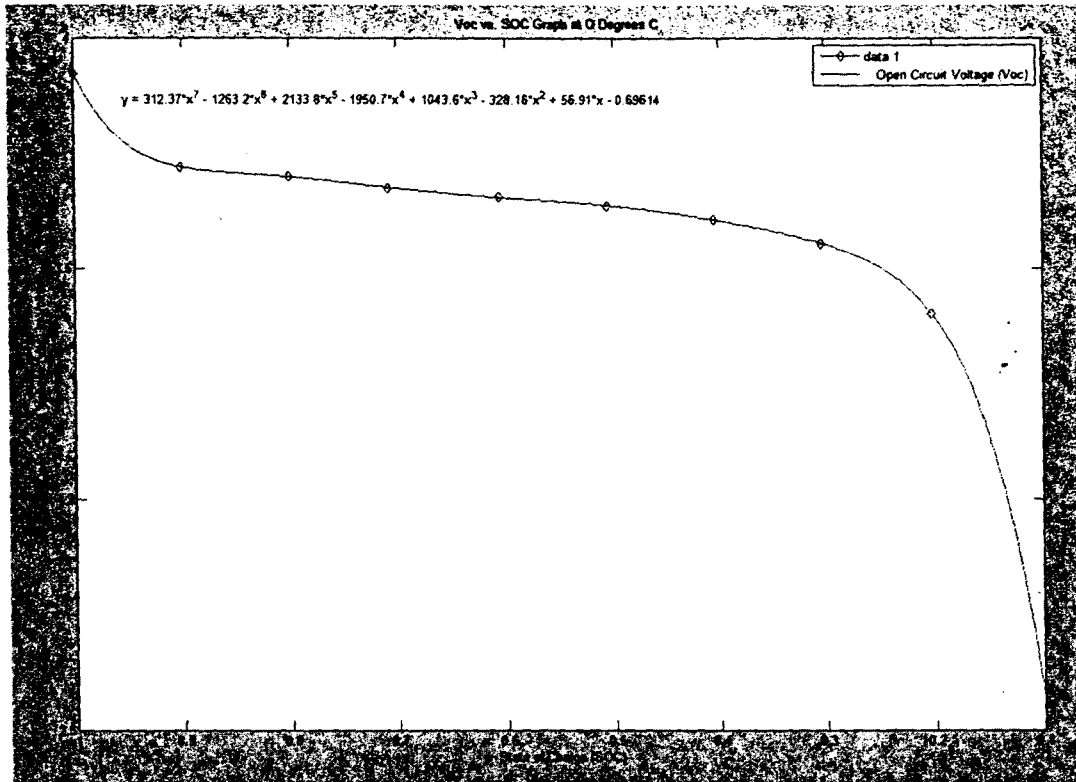


Figure 20:  $V_{oc}$  vs. SOC data points and fitting curves at 0 degrees C

It can be seen that the best fit line crosses majority if not all the data points. The equation provided in the plot is the open circuit voltage equation as a function of SOC. All the individual  $V_{oc}$  vs. SOC plots for their respective temperatures is shown in Appendix 1.4. Figure 20 shows the  $V_{oc}$  vs. SOC plots for all four temperatures and how they compare to their respective data points.

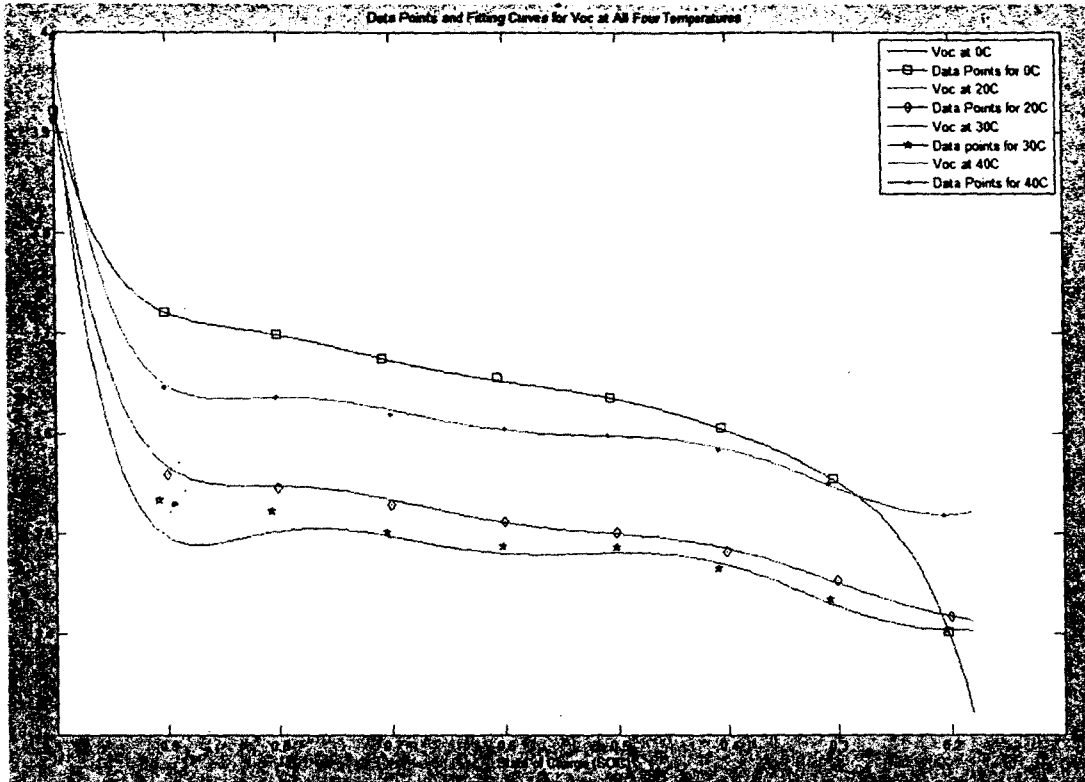


Figure 21: Data points and fitting curves for all four temperatures

Comparing these four graphs, it can be seen that majority of the fitting curves cross their respective data points. The  $V_{oc}$  at 30 degrees C was the only curve did not align perfectly. This occurred because transient data was not provided and  $V_{oc}$  was estimated. That was the most accurate curve to match the data points.

## Discussion

For this thesis, data was analyzed using a mathematical equivalent circuit model in PSCAD. The plots created from the simulation matched the graphs that were constructed from measured values. These simulation results were also verified using MATLAB. The combination of the results found in MATLAB and PSCAD verify that PSCAD is an appropriate tool to use to model the characteristics of a battery.

Observing Figures 12 – 15 it was seen that there was a fairly small marginal error between simulated terminal voltages and the measured terminal voltages. The marginal error for the 0 degree C was approximately 3.8%, the 20 degree C marginal error was 2.3%, the 30 degree C margin was 1.25%, and lastly the 40 degree marginal error was 1.05%. This led to an average error of approximately 2.1%. Table illustrates all of these values.

Temperature (C)	Marginal Error (%)
0	3.8
20	2.3
30	1.25
40	1.05
Average	2.1

Table 5: Marginal temperature for all temperatures

Noting that the graphs have fairly small marginal errors we can conclude that simulating in PSCAD provides valid results.

## **Conclusion and future work**

The modeling of battery characteristics is an extremely important factor in electric vehicle technology. Without good, robust, and reliable batteries this technology will not be able to excel. Being able to simulate how the battery reacts to various temperatures, charging currents, and discharging currents is essential in developing the batteries needed for electric vehicles.

There are a few problems with electric vehicles- for one they can only travel approximately 54 miles before they need to be charged again. This is not suitable for individuals that commute long distances. Another issue is that fully charging these vehicles takes approximately 2-3 hours; this is an inconvenience to some individuals.

In the future, by modeling battery characteristics engineers will be able to find ways to discharge batteries at a lower rate so that cars will be able to travel longer distances. They will also develop a fast charging method that will be able to charge the battery capacity to 80% in 15 minutes or 50 % in 5 minutes. This would be ideal because presently individuals usually spend about 5-10 minutes filling their cars up with gas.

Presently, electric vehicles use various types of batteries in electric vehicles. These batteries include lead acid, lithium ion, lithium polymer, and many others. Recently, the lithium iron phosphate battery has been observed to potentially be suitable for electric vehicles. When compared to a lithium ion battery the lithium iron phosphate battery has shown some improvements and is appropriate for the use of electric vehicles.

This thesis focused on modeling the constant discharging characteristics of a lithium iron phosphate battery using a simulator known as PSCAD. Due to the fact that

PSCAD is only a simulator, MATLAB equations were used to determine resistor, capacitor, and open circuit voltage values. These values were then implemented into PSCAD in order to simulate how the battery operates.

After completing the simulation, the results showed that PSCAD is in fact a reliable and accurate simulator for battery models. The graphs for all four temperatures matched fairly well and only had an average marginal error of approximately 2.1%. The data and graphs were also verified using MATLAB. Due to the combination of both these software's outputting the same data, it can be concluded that PSCAD is a valid and useful tool in modeling batteries.

In the future, the measurements of the charging characteristics of the lithium iron phosphate battery can be analyzed with various temperatures. This will allow for the design of an equivalent circuit that provides both charging and discharging qualities of the battery for numerous temperature conditions. This innovative model can help industries analyze and evaluate the characteristics of a lithium iron phosphate battery in hopes to create a more efficient electric vehicle.

## References

- [1] Salameh, Ziyad M. *Fundamentals of Electric Vehicle Technology*. Print.
- [2] Patel, Dipesh D., Frank P. Tredeau, and Ziyad M. Salameh. *Temperature Effects on Fast Charging Large Format Prismatic Lithium Iron Phosphate Cells. Temperature Effects on Fast Charging Large Format Prismatic Lithium Iron Phosphate Cells*. IEEE. Web. <<http://ieeexplore.ieee.org/stamp/stamp.jsp?arnumber=05729073>>.
- [3] Tredeau, Frank P. *Battery Management Systems*. Thesis. University of Massachusetts Lowell, 2011. Lowell: University of Massachusetts Lowell, 2011. Print.
- [4] Tredeau, Frank P., and Ziyad M. Salameh. *Evaluation of Lithium Iron Phosphate Batteries for Electric Vehicles Application. Evaluation of Lithium Iron Phosphate Batteries for Electric Vehicles Application*. IEEE. Web. <<http://ieeexplore.ieee.org/stamp/stamp.jsp?tp=&arnumber=5289704>>.
- [5] Rao, Ravishankar, Sarma Vrudhula, and Daler N. Rakhmatov. *Battery Modeling for Energy-Aware System Design. Battery Modeling for Energy-Aware System Design*. IEEE. Web. <<http://ieeexplore.ieee.org/stamp/stamp.jsp?tp=&arnumber=1250886>>.
- [6] "PSCAD." *PSCAD*. Manitoba-HVDC Research Centre. Web. <<https://pscad.com/products/pscad>>.
- [7] "Past, Present, & Future." *Past, Present, & Future*. Manitoba-HVDC Research Centre. Web. <[https://pscad.com/products/pscad/past\\_present\\_and\\_future](https://pscad.com/products/pscad/past_present_and_future)>.
- [8] "Extensive Model Libraries." *Model Libraries*. Manitoba-HVDC Research Centre. Web. <[https://pscad.com/products/pscad/extensive\\_model\\_libraries](https://pscad.com/products/pscad/extensive_model_libraries)>.
- [9] "Study of Battery Modeling Using Mathematical and Circuit Oriented Approaches." *Study of Battery Modeling Using Mathematical and Circuit Oriented Approaches*. IEEE. Web. <<http://ieeexplore.ieee.org/stamp/stamp.jsp?arnumber=06039230>>.
- [10] Hu, Tingshu, Brian Zanchi, and Jianping Zhao. *Determining Battery Parameters by Simple Algebraic Method. Determining Battery Parameters by Simple Algebraic Method*. IEEE. Web. <<http://ieeexplore.ieee.org/stamp/stamp.jsp?arnumber=05990614>>.
- [11] Srinivasan, Venkat, and John Newman. *Discharge Model for the Lithium Iron-Phosphate Electrode. Discharge Model for the Lithium Iron-Phosphate Electrode*. ECS. Web. <<http://scitation.aip.org/getpdf/servlet/GetPDFServlet?filetype=pdf&id=JESOAN0001510000100A1517000001&idtype=cvips&prog=normal>>.

- [12] Salameh, Ziyad M., Margaret A. Casacca, and William A. Lynch. *A Mathematical Model for Lead-Acid Batteries. A Mathematical Model for Lead-Acid Batteries*. IEEE. Web. <<http://ieeexplore.ieee.org/stamp/stamp.jsp?arnumber=00124547>>.
- [13] Lynch, W. A., and Ziyad M. Salameh. *Electrical Component Model for a Nickel-Cadmium Electric Vehicle Traction Battery. Electrical Component Model for a Nickel-Cadmium Electric Vehicle Traction Battery*. IEEE. Web. <<http://ieeexplore.ieee.org/stamp/stamp.jsp?arnumber=01709569>>.
- [14] Botte, Gerardine G. *Mathematical Modeling of Secondary Lithium Batteries. Mathematical Modeling of Secondary Lithium Batteries*. Pergamon. Web. <[http://iweb.tntech.edu/vsubramanian/pubs/4-EActa-GB-VS-RW-mathmodeling\\_sec\\_Lith\\_bat-2000.pdf](http://iweb.tntech.edu/vsubramanian/pubs/4-EActa-GB-VS-RW-mathmodeling_sec_Lith_bat-2000.pdf)>.
- [15] Mischinger, Stefan, Kai Strunz, and Johannes Eckstein. *Modeling and Evaluation of Battery Electric Vehicle Usage by Commuters. Modeling and Evaluation of Battery Electric Vehicle Usage by Commuters*. IEEE. Web. <<http://ieeexplore.ieee.org/stamp/stamp.jsp?tp=&arnumber=6039645>>.
- [16] Rong, Peng, and Massoud Pedram. *An Analytical Model for Predicting the Remaining Battery Capacity of Lithium-Ion Batteries. An Analytical Model for Predicting the Remaining Battery Capacity of Lithium-Ion Batteries*. IEEE. Web. <<http://ieeexplore.ieee.org/stamp/stamp.jsp?tp=&arnumber=1650223>>.
- [17] Gao, Lijun, Shengyi Liu, and Roger A. Dougal. *Dynamic Lithium-Ion Battery Model for System Simulation. Dynamic Lithium-Ion Battery Model for System Simulation*. IEEE. Web. <<http://ieeexplore.ieee.org/stamp/stamp.jsp?tp=&arnumber=1159187>>.
- [18] Kuhn, E., C. Forgez, P. Lagonotte, and G. Friedrich. *Modelling Ni-mH Battery Using Cauer and Foster Structures. Modelling Ni-mH Battery Using Cauer and Foster Structures*. IEEE. Web. <<http://www.sciencedirect.com/science/article/pii/S0378775305014096>>.
- [19] C. Alaoui, Z. Salameh, and W. Lynch, "Sealed Lead Acid Electric Vehicle Batteries: A Performance Comparison Study", International Journal of Power and Energy Systems Vol. 21, No 3, PP. 174-180, 2001.
- [20] W. Lynch and Z. Salameh, "Rechargeability and Characteristics of Flat Type Zinc Manganese Batteries", Proceedings of the IEE North American Power Symposium, Boston, MA., Nov. 9-10, 1996.

[21] W. Lynch and Z. Salameh, "Electrical Component Model for a Nickel Cadmium Electric Vehicle Traction Battery," Annual IEEE\_PES, PP. NO, 06GM1201, Montreal, Canada, 2006

[22]F. Tradeau and Z. Salameh, "Characterization of the M100-12 NiZn Battery IASTED, Jan. Orlando, Fl.2007.

[23] Kim Bong, F. Tradeau and ZiyadSalameh, "Fast Chargeability of Lithium Polymer Batteries". Annual IEEE\_PES Meeting, PP. NO, 08GM0857.

[24] Kim Bong, F. Tradeau and ZiyadSalameh, "Performance Evaluation of Lithium Polymer batteries for use in Electric vehicles". VPPC 2008 Harbin, Sep 3-7, China.

[25] Kim Bong, and ZiyadSalameh, "Advanced Lithium Polymer Batteries", IEEE PES GM09 to be presented in July in Calgary, Canada.

**Appendix 1.1**

Soc vs Voc at 20 Degrees C	
SOC	VOC
1	3.914
0.9	3.559
0.8	3.546
0.7	3.529
0.6	3.512
0.5	3.501
0.4	3.482
0.3	3.453
0.2	3.417
0.1	3.376

Soc vs Voc at 0 Degrees C	
SOC	VOC
1	3.922
0.9	3.7205
0.8	3.6993
0.7	3.675
0.6	3.6558
0.5	3.6359
0.4	3.606
0.3	3.5547
0.2	3.4024
0.1	Not Provided

Soc vs Voc at 30 Degrees C	
SOC	VOC
1	3.996
0.9	3.533
0.8	3.5226
0.7	3.5008
0.6	3.4873
0.5	3.4861
0.4	3.4651
0.3	3.4348
0.2	3.403
0.1	3.37

Soc vs Voc at 40 Degrees C	
SOC	VOC
1	3.9778
0.9	3.646
0.8	3.636
0.7	3.619
0.6	3.605
0.5	3.598
0.4	3.584
0.3	3.55
0.2	3.518
0.1	3.5586

## Appendix 1.2

R1 Values for All Temperatures	
Temperature (C)	R1( $\Omega$ )
0	0.00136
20	0.00305
30	0.0031375
40	0.002325

C1 Values for All Temperatures	
Temperature (C)	C1 (F)
0	44117.65
20	39344.26
30	38247.01
40	51612.9

R2 Values for All Temperatures	
Temperature (C)	R2 ( $\Omega$ )
0	0.0007375
20	0.000925
30	0.0013
40	0.001275

C2 Values for All Temperatures	
Temperature (C)	C2 (F)
0	162711.86
20	129729.73
30	92307.69
40	94117.65

R3 Values for All Temperatures	
Temperature(C)	R3( $\Omega$ )
0	0.000425
20	0.0003375
30	0.000525
40	0.00055

C3 Values for All Temperatures	
Temperature(C)	C3 (F)
0	988235.29
20	711111.11
30	571428.57
40	654545.45

### Appendix 1.3

#### **Matlab Code for Simulated Terminal Voltage at 0 Degrees C:**

```
R1= 0.00136;  
R2=0.0007375;  
R3=0.000425;  
C1=44117.65;  
C2=162711.86;  
C3=988235.29;  
t= 0:60:3000;  
I=80;
```

```
Vt= 3.922 - (R1*I*(1-exp(-t/(R1*C1)))) - (R2*I*(1-exp(-t/(R2*C2)))) -  
(R3*I*(1-exp(-t/(R3*C3))));
```

#### **Matlab Code for Simulated Terminal Voltage at 20 Degrees C:**

```
R1= 0.00305;  
R2=0.000925;  
R3=0.0003375;  
C1=39344.26;  
C2=129729.73;  
C3=711111.11;  
t= 0:60:3000;  
I=80;
```

```
Vt= 3.914 - (R1*I*(1-exp(-t/(R1*C1)))) - (R2*I*(1-exp(-t/(R2*C2)))) -  
(R3*I*(1-exp(-t/(R3*C3))));
```

#### **Matlab Code for Simulated Terminal Voltage at 30 Degrees C:**

```
R1= 0.0031375  
R2=0.0013;  
R3=0.000525;  
C1=38247.01;  
C2=92307.69;  
C3=571428.57;  
t= 0:60:3000;  
I=80;
```

```
Vt= 3.996 - (R1*I*(1-exp(-t/(R1*C1)))) - (R2*I*(1-exp(-t/(R2*C2)))) -  
(R3*I*(1-exp(-t/(R3*C3))));
```

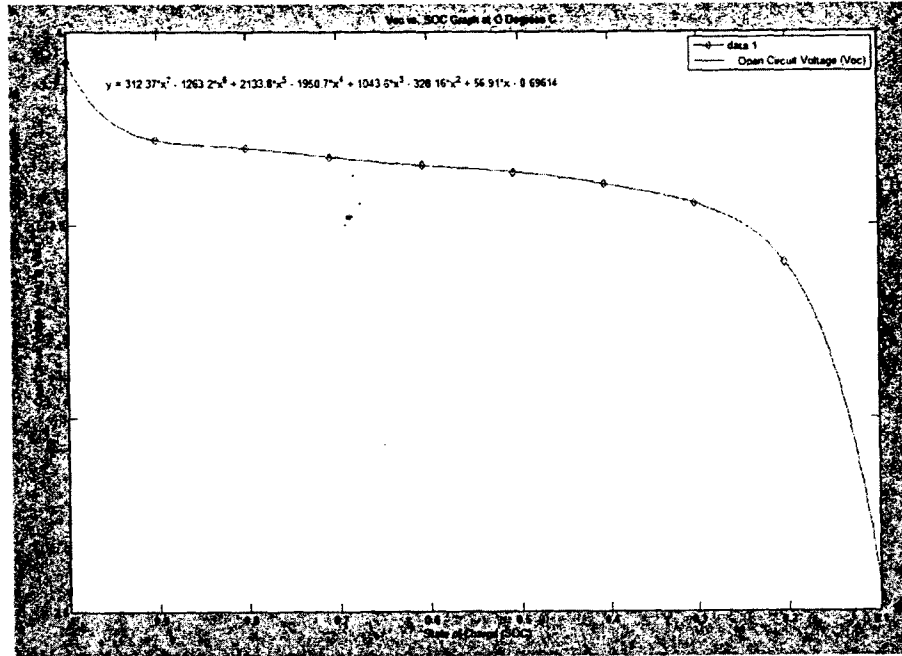
### Matlab Code for Simulated Terminal Voltage at 40 Degrees C:

```
R1= 0.002325;  
R2=0.001275;  
R3=0.00055;  
C1=51612.9;  
C2=94117.65;  
C3=654545.45;  
t= 0:60:3000;  
I=80;
```

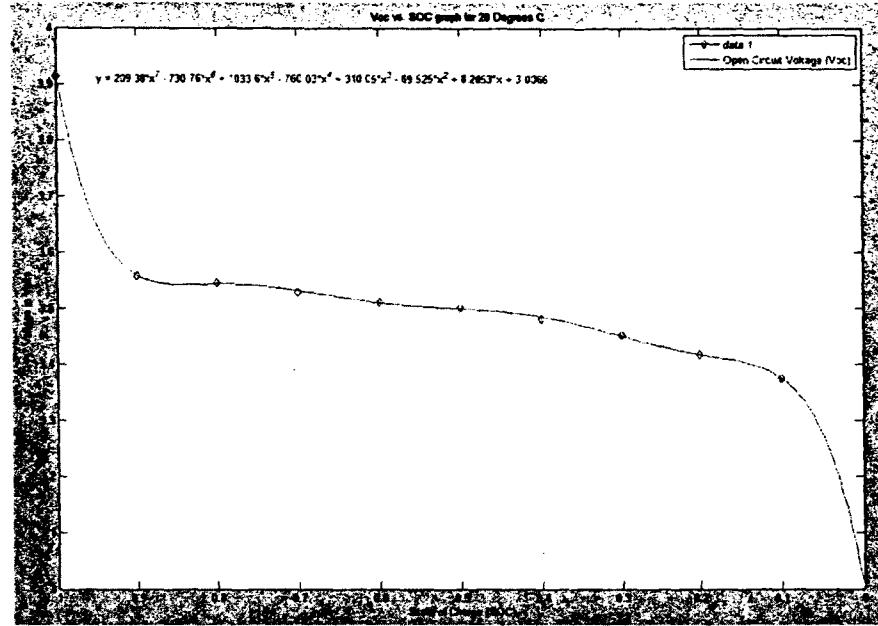
```
Vt= 3.9778 - (R1*I*(1-exp(-t/(R1*C1)))) - (R2*I*(1-exp(-t/(R2*C2)))) -  
(R3*I*(1-exp(-t/(R3*C3))));
```

## Appendix 1.4

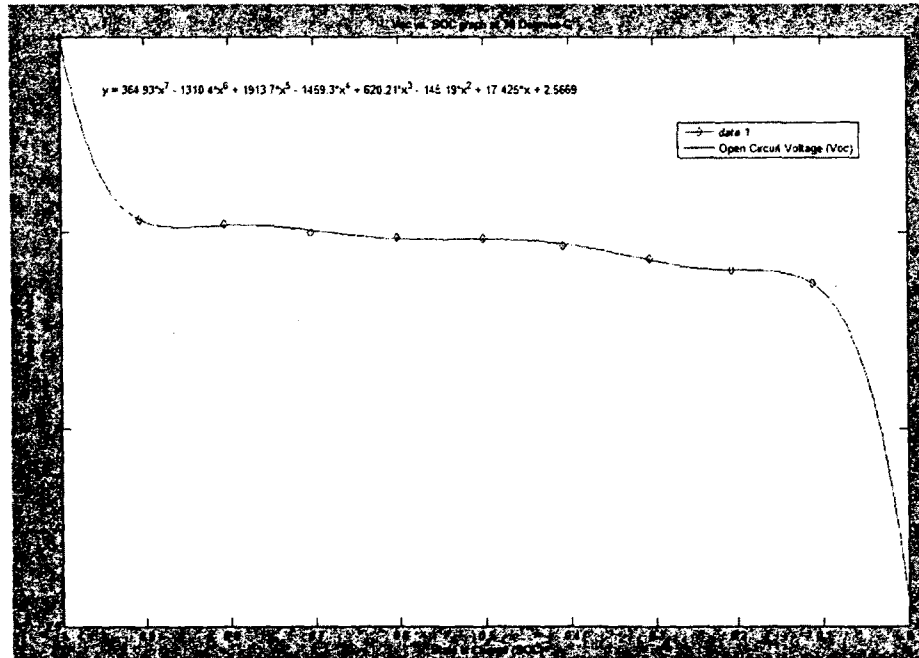
$V_{oc}$  vs. SOC data points and fitting curves at 0 degrees C:



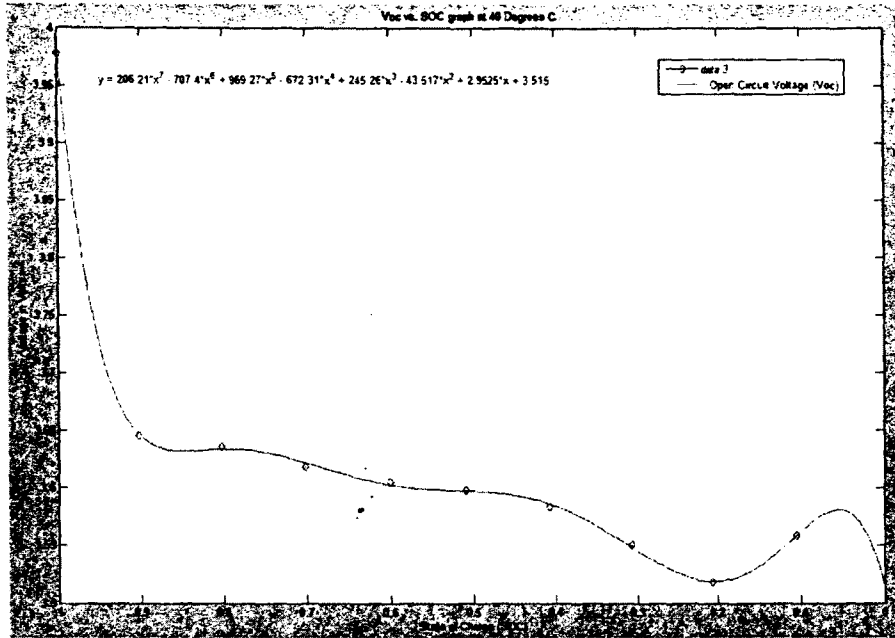
$V_{oc}$  vs. SOC data points and fitting curves at 20 degrees C:



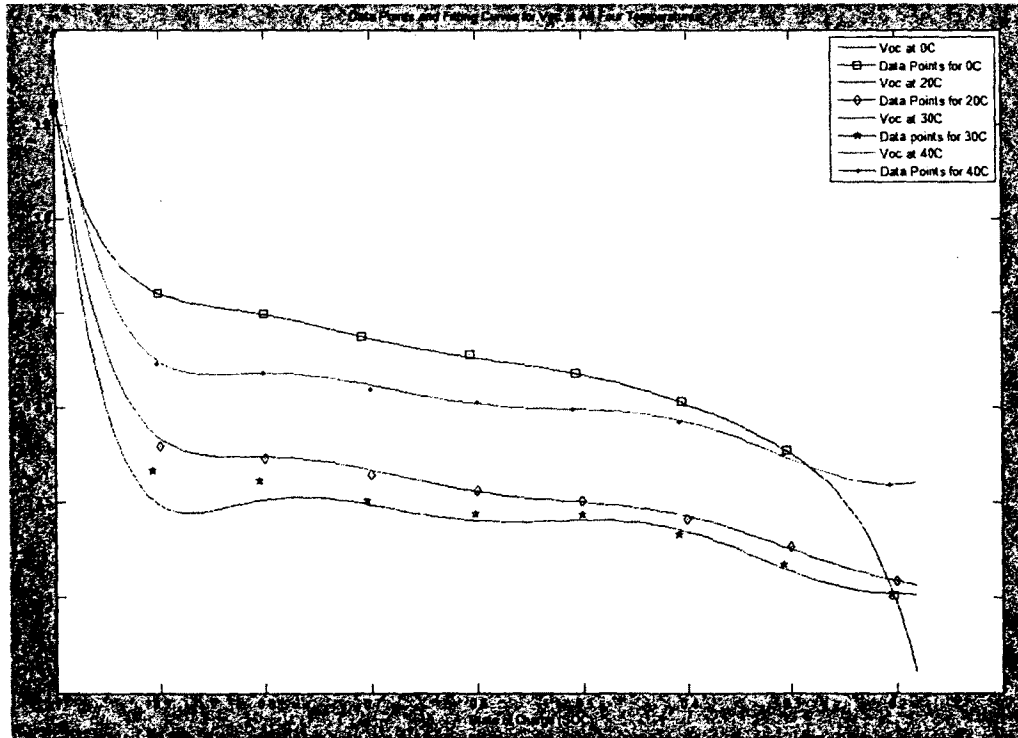
**V<sub>oc</sub> vs. SOC data points and fitting curves at 30 degrees C:**



**V<sub>oc</sub> vs. SOC data points and fitting curves at 40 degrees C:**



All four temperatures  $V_{oc}$  vs. SOC data points and fitting curves:



## **Biography**

**Garo Yessayan** was born in Jamaica Plain, Massachusetts. He attended high school at Boston Latin School. He was a co-captain for his high school football and wrestling teams. Once graduating high school, he was accepted to the electrical engineering program at the University of Massachusetts Lowell. At UMass Lowell, he became a resident adviser and a member of the club rugby team. He received his B.S.E.E at the University of Massachusetts Lowell in 2011 and is currently pursuing his M.S.E.E. at UMass Lowell. His areas of interest are renewable energy and power electronics.